Enzymatic Synthesis and Polymerization of Saccharide-Vinyl Monomers in Aqueous Systems

Adharis, Azis

Chapter 3

Environmentally Friendly Pathways Towards the Synthesis of Vinyl-Based Oligocelluloses

The synthesis of vinyl-based oligocelluloses using cellodextrin phosphorylase as biocatalyst in buffer solution is presented. Various types of vinyl glucosides bearing (meth)acrylates/(meth)acrylamides functionalities served as the glucosyl acceptor in the enzyme catalyzed reverse phosphorolysis reaction and α-glucose 1-phosphate as the glucosyl donor. The enzymatic reaction was followed by thin layer chromatography and the isolated product yields were about 65%. The synthesized vinyl-based oligocelluloses had an average number of repeating glucosyl units and a number average molecular weight up to 8.9 and 1553 g mol^{-1}, respectively. The majority of the bonds at the alpha position of acrylate units in (β-oligocellulosyloxy)ethyl acrylate was fragmented as characterized by ^{1}H NMR spectroscopy and MALDI-ToF mass spectrometry. Nevertheless, a minor amount of fragmentation was observed in (β-oligocellulosyloxy)ethyl methacrylate and (β-oligocellulosyloxy)butyl acrylate but no fragmentation was detected in the (meth)acrylamide-based oligocelluloses. Crystal lattice of the prepared vinyl-based oligocelluloses was investigated *via* wide-angle X-ray diffraction experiments.

This chapter was published in: *Carbohydr. Polym.* **2018**, *193*, 196–204.

3.1 Introduction

Cellulose is the most abundant biopolymer on earth and has been widely used in our daily lives mainly for paper products, composites, and building materials.[1–5] Cellulose is a linear polymer which consists of a hundred to a thousand glucosyl units linked through β-(1→4)-glycosidic bonds. Cellulose oligomers or cellooligosaccharides, later mentioned as oligocelluloses, typically contain only a few glucosyl units and gained some interest in the last decades especially because of their properties which are essentially the same as natural cellulose. Besides, these materials have potential applications for non-digestible dietary fiber products,[6–9] novel biobased surfactants,[10–12] hybrid nanomaterials,[13,14] and scaffold candidates for tissue engineering.[15]

In general, two methods have been utilized to obtain oligocelluloses: (1) Degradation of natural cellulose and (2) synthetic pathways *via* chemical or enzymatic reactions.[16] The first method is easy to be performed since it just requires relatively cheap acidic reagents, however, this route has less control over the chemical and crystalline structures of the products. In addition, not only oligocelluloses but also unwanted furanic by-products will be formed rendering fractionation/purification steps of the reaction mixture necessary. The chemical synthesis is based on ring-opening polymerization of structurally modified glucopyranoses[17,18] and glucosylation reactions between glucosyl donors and glucosyl acceptors.[10,19] Even though well-defined oligomers with high purity can be achieved, these approaches are time-consuming due to multi-step reactions involved in the precursor's synthesis.

I*n vitro* enzymatic synthesis of oligocelluloses provides some advantages compared to the previous methods; for example, well-controlled structures of products are obtained in a one-step polymerization owing to high regio-, enantio-, chemo-, and stereoselectivities of the enzymes. Moreover, enzymes are non-toxic compounds, isolated from sustainable resources, and catalyze the reaction under mild environments.[20–23]

Cellulases[24–26] and cellodextrin phosphorylases (CdP's)[27–29] are the most exploited enzymes for the production of synthetic oligocelluloses. Cellulases can catalyze the polycondensation reaction of β-cellobiosyl fluorides and the reaction is necessarily performed in organic solvent/buffer mixtures to maintain the products solubility and to prevent the products hydrolysis – facilitated by the enzyme itself. On the other hand, CdP's are able to accept a broader range of substrates such as glucose,[30,31] cellobiose,[32,33] and various cellodextrins[34] for the synthesis of oligocelluloses *via* a reverse phosphorolysis mechanism in aqueous media. The effort to apply unnatural substrates for CdP from

Clostridium thermocellum (CtCdP) was first studied by Serizawa and coworkers.[15,35–38] They utilized monofunctional glucose, in which the anomeric carbon was chemically bonded either with alkyl, amine, azide, oligo(ethylene glycol) or methacrylate groups in order to provide additional reactivities of the prepared oligocelluloses with other molecules or to control their self-assembly processes.

In this report, we extend the range of structures reported and present different novel types of vinyl glucosides – (β-glucosyloxy)ethyl acrylate, (β-glucosyloxy)ethyl methacrylate, (β-glucosyloxy)butyl acrylate, (β-glucosyloxy)ethyl acrylamide, and (β-glucosyloxy)ethyl methacrylamide – as promising substrates for CtCdP in the synthesis of vinyl-based oligocelluloses whereby α-glucose 1-phosphate served as the glucosyl donor. The used vinyl glucosides, that were uniquely characterized to be anomerically pure and monofunctional, were synthesized enzymatically under environmentally benign conditions.[39,40] In addition, the hydroxyalkyl (meth)acrylates/(meth)acrylamides, the source of the vinyl groups, can be synthesized using biobased precursors of acrylic acid,[41] methacrylic acid,[42] and ethylene glycols.[43] Hence, the overall reaction can be considered as a green route towards the production of vinyl-based oligocelluloses, which is due to the choice of starting materials, catalysts, and solvent. The starting materials were derived from renewable feedstocks, whereas enzymes were used as the biocatalyst and the utilized solvent was a water based buffer solution. Furthermore, vinyl groups available at the reducing end of the oligocelluloses offer high reactivity and versatility for further (co)polymerization with different monomers, resulting in polymers with novel physical and chemical properties. For instance, the synthesized (co)polymers can be applied as promising biobased materials like hydrogels,[15,44,45] polymeric surfactants,[46,47] compatibilizer,[48] and as well-defined nanostructure materials.[49–51] The synthesized vinyl-based oligocelluloses were successfully characterized by proton nuclear magnetic resonance spectroscopy, size exclusion chromatography, wide-angle X-ray diffraction, and matrix-assisted laser desorption/ionization time-of-flight mass spectrometry.

3.2 Experimental

An experimental roadmap for the synthesis and characterization of the vinyl-based oligocelluloses is presented in Figure 3.1. The materials used for the synthesis, the characterization methods, as well as the synthetic procedure are outlined in the following paragraphs.

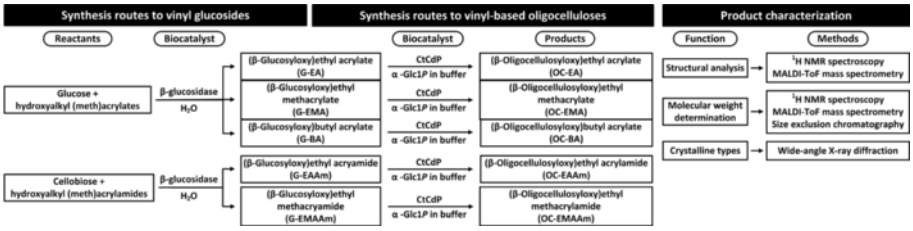

Figure 3.1 Synthesis and characterization roadmap of the vinyl-based oligocelluloses.

3.2.1 Materials

α-D-Glucose 1-phosphate disodium salt hydrate ≥97% (α-Glc1*P*) and *n*-butanol (*n*-BuOH) were purchased from Sigma-Aldrich. Cellobiose 98% was purchased from Acros Organics. Ethanol (EtOH), isopropyl alcohol (IPA), and concentrated H_2SO_4 were acquired from Avantor. Unless otherwise mentioned, all chemicals were used as received. Five types of vinyl glucosides consist of 2-(β-glucosyloxy)ethyl acrylate (G-EA), 2-(β-glucosyloxy) ethyl methacrylate (G-EMA), 4-(β-glucosyloxy)butyl acrylate (G-BA), *N*-(β-glucosyloxy) ethyl acrylamide (G-EAAm), and *N*-(β-glucosyloxy)ethyl methacrylamide (G-EMAAm) were synthesized according to the literature.[39,40] CtCdP was expressed in *Escherichia coli* BL21-Gold-(DE3) strain harboring pET28a-CtCdP plasmid and purified as reported before.[33] The activity of the enzyme was 15.2 units per mL of stock solution, equal to 0.13 units per mL of the reaction mixture (One unit was defined as the amount of enzyme that converts 1μmol of substrate per minute under HEPES buffer pH 7.5 at 45 °C).

3.2.2 Characterization

Thin Layer Chromatography (TLC). TLC was carried out on aluminum sheet silica gel 60/kieselguhr (Merck) using eluent of *n*-BuOH/IPA/H_2O (1/2.5/1.5). Spot visualization of the products was performed by spraying the TLC plate with 5% H_2SO_4 in EtOH followed by heating.

^{1}H nuclear magnetic resonance (NMR) spectroscopy. ^{1}H NMR spectra were recorded on a 400 MHz Varian VXR Spectrometer using 4 wt% sodium deuteroxide (Aldrich) in deuterium oxide (99.9 atom % D, Aldrich) as the solvent. The acquired spectra were processed by MestReNova Software from Mestrelab Research S.L.

The average degree of polymerization (DP_n) of the vinyl-based oligocelluloses was calculated from the ^{1}H NMR spectra (Figure 3.3) using equation 3.1 while DP_n of the native oligocellulose was determined using equation 3.2. *H*1, *H*2, and $H11_{trans}$ represent the peak integration of anomeric proton on C-1 position, proton on C-2 position, and one of the protons of the vinyl groups in the vinyl-based oligocelluloses, respectively. Furthermore,

Hα and *Hβ* are equal to the peak integration of alpha-anomeric and beta-anomeric protons of the native oligocellulose.

$$DP_n = \frac{H1+H2}{H11_{trans}} \quad (3.1)$$

$$DP_n = \frac{H\alpha+H\beta+H2}{H\alpha+H\beta} \quad (3.2)$$

The number–average molecular weight (M_n) of the vinyl-based and native oligocelluloses were determined *via* equation 3.3 where M_o and B are the molecular weights of dehydrated glucose and hydroxy-alkyl (meth)acrylate/(meth)acrylamide units (or water molecule), respectively.

$$M_n = (DP_n \times M_o) + B \quad (3.3)$$

Matrix-Assisted Laser Desorption/Ionization Time-of-Flight Mass Spectrometry (MALDI-ToF MS). MALDI-ToF MS was executed on a Voyager DE-PRO instrument from Applied Biosystems in the positive and linear mode. In a MALDI-ToF MS plate, 0.5 µL of oligocellulose suspensions (2–5 mg mL^{-1}) was mixed with 1.0 µL of matrix solution (10 mg of 2,5-dihydroxybenzoic acid in 1 mL of 50 v% H_2O, 50 v% acetonitrile, 0.01 v% trifluoroacetic acid). The obtained spectra were analyzed using Data Explorer Software from Applied Biosystems.

Weight–average molecular weight (M_w), M_n, and dispersity ($Đ$) of the vinyl-based and native oligocelluloses were determined from the MALDI-ToF spectra (Figure 3.4) by equation 3.4–3.6, respectively, where N_i and M_i refer to the area below the peak and the molar mass of the i-th oligocellulose species.

$$M_n = \frac{\sum_i(N_i M_i)}{\sum_i(N_i)} \quad (3.4)$$

$$M_w = \frac{\sum_i(N_i M_i^2)}{\sum_i(N_i M_i)} \quad (3.5)$$

$$Đ = \frac{M_w}{M_n} \quad (3.6)$$

Size Exclusion Chromatography (SEC). SEC was done on an Agilent Technologies 1260 Infinity from PSS (Mainz, Germany) and DMSO containing 0.05 M LiBr was used as the eluent with the flow rate of 0.5 mL min^{-1}. The SEC was equipped with three detectors (a refractive index detector G1362A 1260 RID from Agilent Technologies at 45 °C, a viscometer detector ETA-2010 from PSS at 60 °C, and a multiangle laser light scattering detector SLD

7000 from PSS at room temperature. The samples were injected with a flow rate of 0.5 mL min^{-1} into an MZ Super-FG 100 SEC column and two PFG SEC columns 300 and 4000 at a temperature of 80 °C. The samples were filtered through a 0.45 µm PTFE filter prior to injection. Pullulan standards with the M_w ranging from 342 to 805000 g mol^{-1} were used for calibration and molecular weights of the samples were calculated by standard calibration method using WinGPC Unity Software from PSS.

Wide-Angle X-ray Diffraction (WAXD). WAXD was carried out using Bruker D8 Advance diffractometer (Cu Kα radiation, λ = 0.1542 nm) in the angular range of 5–50° (2θ) at room temperature. The Miller indices of synthetic vinyl-based and native oligocelluloses were assigned following the literature.[35]

3.2.3 *In vitro* synthesis of vinyl-based and native oligocelluloses

In a 50 mL falcon tube was dissolved α-Glc1*P* (1.82 g, 6.0 mmol) in 30 mL HEPES buffer 500 mM, pH 7.5, at room temperature. Subsequently, 0.3 mmol of G-EA (83.4 mg), G-EMA (87.6 mg), G-BA (96 mg), G-EAAm (83.1 mg), G-EMAAm (87.3 mg), or cellobiose (102.7 mg) was added into the α-Glc1*P* solution. The reaction was started by adding the enzyme solution (250 µL) and putting the tube on Eppendorf Thermomixer comfort (45 °C, 600 rpm, 72 h). After few hours, the white turbid solution was observed. The reaction products were isolated by centrifugation on Thermo Scientific Heraeus Labofuge 400 R (4500 rpm, 20 min, 4 °C) and the precipitates were washed at least three times with Milli-Q water. The products were then lyophilized in a freeze-drier (-45 °C, 0.01 mbar) overnight. The product yields were calculated by comparing the isolated product weights with the theoretical product weights (the obtained M_n from MALDI-ToF MS measurements was used for the calculation of theoretical weights).

(β-Oligocellulosyloxy)ethyl methacrylamide (OC-EMAAm). White powder, 280 mg, yield: 70%. ^{1}H NMR (4 wt% NaOD/D_2O) δ in ppm: 5.51 (H11-*cis*), 5.26 (H11-*trans*), 4.26 (H2, *J* = 7.8 Hz), 4.18 (H1, *J* = 7.6 Hz), 3.03–3.81 (H3, H4, H5, H6, H7, H8, H9), 1.73 (H12).

(β-Oligocellulosyloxy)ethyl acrylamide (OC-EAAm). White powder, 248 mg, yield: 63%. ^{1}H NMR (4 wt% NaOD/D_2O) δ in ppm: 5.96–6.13 (H11-cis and H10), 5.56 (H11-trans, *J* = 11.6 Hz), 4.25 (H2, *J* = 8.0 Hz), 4.16 (H1, *J* = 8.0 Hz), 3.01–3.82 (H3, H4, H5, H6, H7, H8, H9).

(β-Oligocellulosyloxy)butyl acrylate (OC-BA). White powder, 239 mg, yield: 58%. ^{1}H NMR (4 wt% NaOD/D_2O) δ in ppm: 5.74–5.91 (H11-cis and H10), 5.41 (H11-trans, *J* = 12 Hz), 4.21 (H2, *J* = 8.2 Hz), 4.14 (H1, *J* = 8.0 Hz), 2.97–3.67 (H3, H4, H5, H6, H7, H8, H9), 1.31–1.45 (H8', H9').

(β-Oligocellulosyloxy)ethyl methacrylate (OC-EMA). White powder, 298 mg, yield: 67%. ^{1}H NMR (4 wt% NaOD/D_2O) δ in ppm: 5.46 (H11-*cis*), 5.15 (H11-*trans*), 4.26 (H2, *J* = 7.8 Hz), 4.20 (H1, *J* = 8.0 Hz), 3.02–3.78 (H3, H4, H5, H6, H7, H8, H9), 1.67 (H12).

(β-Oligocellulosyloxy)ethyl acrylate (OC-EA). White powder, 304 mg, yield: 65%. ^{1}H NMR (4 wt% NaOD/D_2O) δ in ppm: 5.78–5.96 (H11-cis and H10), 5.45 (H11-trans, *J* = 11.6 Hz), 4.26 (H2, *J* = 8.0 Hz), 4.19 (H1, *J* = 7.6 Hz), 3.02–3.78 (H3, H4, H5, H6, H7, H8, H9).

Native oligocellulose (OC). White powder, 231 mg, yield: 66%. ^{1}H NMR (4 wt% NaOD/D_2O) δ in ppm: 5.11 (Hα), 4.53 (Hβ, *J* = 7.2 Hz), 4.28 (H2, *J* = 8.2 Hz), 3.04–3.74 (H3, H4, H5, H6, H7).

3.2.4 Optimization reaction condition

Three 50 mL of falcon tubes were prepared and different amount of α-Glc1*P* was added into each tube (0.91 g, 3.0 mmol; 1.82 g, 6.0 mmol; 3.64 g, 12.0 mmol) then dissolved by 30 mL HEPES buffer 500 mM, pH 7.5, at room temperature. Subsequently, G-EA (83.4 mg, 0.30 mmol) was added to the α-Glc1*P* solution. The reaction was started by adding the enzyme solution (250 µL) and putting the tubes in an Eppendorf Thermomixer comfort (45 °C, 600 rpm). After certain time intervals, TLC of the reaction mixture was performed and the reaction product was detected at retardation factor of 0.63.

3.3 Results and discussion

3.3.1 Synthesis of vinyl-based and native oligocelluloses

Cellodextrin phosphorylase (CdP, EC 2.4.1.49) is a member of the glycoside hydrolase family 94 and it is known to be able to catalyze both phosphorolysis and synthesis of oligocelluloses in a stereospecific fashion.[52] CdP has high substrate promiscuity that gave us an opportunity to use not only its natural substrates but also unnatural substrates as the glucosyl acceptors in the reactions. For instance, Soetaert and coworkers reported the CdP from *Clostridium stercorarium* can catalyze the reaction with aryl- and alkyl β-glucosides as well as gluco- and sophorolipids served as the substrate.[53,54] In our study, a recombinant CdP from *Clostridium thermocellum* (CtCdP) was employed to catalyze the synthesis of vinyl-based oligocelluloses *via* reverse phosphorolysis mechanism as shown in Scheme 3.1b. The enzymatic synthesis of vinyl-based oligocelluloses used vinyl glucosides as the glucosyl acceptors and α-glucose 1-phosphate (α-Glc1*P*) as the glucosyl donor and the reaction was carried out in buffer media. The glucosides contain (meth)acrylate/(meth)acrylamide groups that are exclusively bond to the anomeric carbon of glucose at the beta configuration and these compounds were also synthesized enzymatically (Scheme 3.1a) using commercial β-glucosidase in aqueous environments as described before.[39,40]

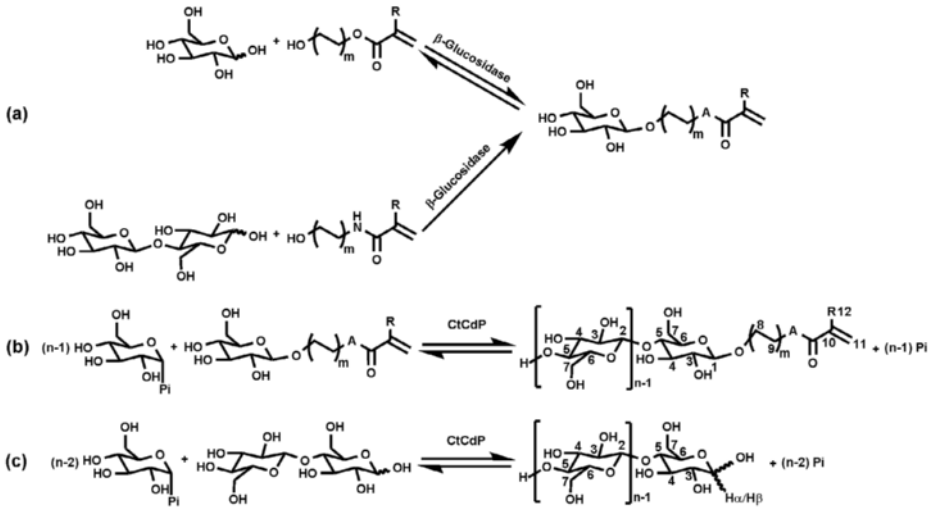

Scheme 3.1 Enzymatic synthesis of (a) vinyl glucosides catalyzed by β-glucosidase, (b) vinyl-based and (c) native oligocelluloses catalyzed by CtCdP (m, A, and R are enlisted in Table 3.1).

Five types of vinyl-based oligocelluloses were successfully synthesized from the corresponding vinyl glucosides: (β-Oligocellulosyloxy)ethyl acrylate (OC-EA), (β-oligocellulosyloxy)ethyl methacrylate (OC-EMA), (β-oligocellulosyloxy)butyl acrylate (OC-BA), (β-oligocellulosyloxy)ethyl acrylamide (OC-EAAm), and (β-oligocellulosyloxy) ethyl methacrylamide (OC-EMAAm). Furthermore, we also synthesized native oligocellulose using cellobiose as the natural substrate (see scheme 3.1c) in order to compare the characteristic of the synthesized vinyl-based oligocelluloses with the native ones. The transparent reaction mixtures upon catalysis by CtCdP became turbid, suggesting that water-insoluble products were formed during the synthesis of vinyl-based and native oligocelluloses. In contrast, the control reaction (without enzyme) remains transparent after three days confirming the role of the enzyme in the catalysis of the reactions. The reaction products were separated from the unreacted α-Glc1*P* and the biocatalyst by centrifugation and the precipitates were washed few times with water resulting in the isolated product yields from 58% to 70%.

Table 3.1 Overview of the enzymatically-synthesized vinyl-based and native oligocelluloses.

Substrate names	m/A/R	Product names	^{1}H NMR		MALDI-ToF MS				SEC			
			M_n	DP_n	M_n	M_w	$Đ$	DP_n	M_n	M_w	$Đ$	DP_n
G-EMAAm	1/NH/CH_3	OC-EMAAm	1435	8.1	1326	1443	1.09	7.4	1460	1587	1.09	8.2
G-EAAm	1/NH/H	OC-EAAm	1335	7.5	1310	1323	1.01	7.4	1460	1570	1.08	8.3
G-BA	2/O/H	OC-BA	1327	7.3	1385	1413	1.02	7.7	1512	1632	1.08	8.4
G-EMA	1/O/CH_3	OC-EMA	1475	8.3	1492	1520	1.02	8.4	1504	1609	1.07	8.5
G-EA	1/O/H	OC-EA	3483	20.8	1553	1647	1.06	8.9	1385	1483	1.07	7.8
Cellobiose	-	OC	1138	6.9	1170	1195	1.02	7.1	1155	1220	1.06	7.0

Number–average molecular weight (M_n) and weight–average molecular weight (M_w) in g mol^{-1}.

Product formation of the enzymatic synthesis of OC-EA was followed by TLC using eluent mixtures of *n*-BuOH/IPA/H_2O. TLC analysis of the reaction mixtures was performed at different time intervals and different α-Glc1*P* concentrations. Figure 3.2 shows that during the period of 72 h, spots belonging to the reaction product clearly appeared at a retardation factor of 0.63 whereas the spots of the glucosyl acceptor were diminished. According to the TLC results, all G-EA (10 mM) were completely reacted with α-Glc1*P* in the mentioned reaction conditions. Visual comparison of the product spots on TLC after 72 h reaction shows that the reaction condition with 200 mM α-Glc1*P* (Figure 3.2b) resulted in a stronger spot intensity than the reaction condition with 100 mM (Figure 3.2a). Besides this, the spots corresponding to the unreacted α-Glc1*P* were found to be more intense in the reaction with 400 mM (Figure 3.2c) as compared with 200 mM (Figure 3.2b). Based on these results, we concluded that the optimal reaction conditions were achieved when the concentration of glucosyl donor was twenty times the concentration of glucosyl acceptor. Therefore, this reaction condition was used for the synthesis of all other vinyl-based and native oligocelluloses.

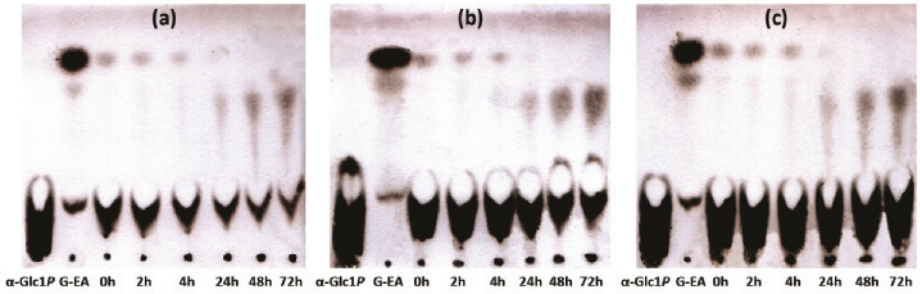

Figure 3.2 TLC analysis of OC-EA synthesis with 10 mM G-EA and [α-Glc1*P*] of (a) 100 mM, (b) 200 mM, and (c) 400 mM at different reaction time intervals catalyzed by CtCdP.

3.3.2 Characterization and fragmentation phenomena

Figure 3.3a shows ^{1}H NMR spectra of the enzymatically synthesized vinyl-based and native oligocelluloses with protons designated as in Scheme 3.1b and 3.1c. Anomeric proton peaks of vinyl glucosides (H1) at 4.14–4.20 ppm and internal anomeric proton peaks (H2) of glucosyl repeating units at 4.21–4.26 ppm were clearly recognized, suggesting that the glucosyl units were successfully linked at the non-reducing end of the vinyl glucosides. In contrast to native oligocellulose, no α and β-anomeric proton peaks (Hα & Hβ) were detected in the spectra of vinyl-based oligocelluloses. Furthermore, the proton peaks at 5.15–6.13 ppm correspond to vinyl protons (H10 & H11) of the substrates. Both results reveal that the alkyl-(meth)acrylate/(meth)acrylamide sequences continue to exist at the reducing end of the oligocelluloses after the enzymatic reaction.

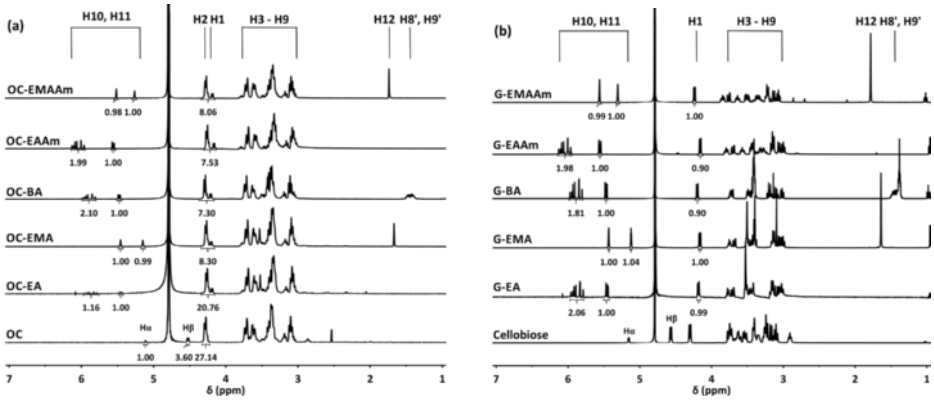

Figure 3.3 ^{1}H NMR spectra of (a) the synthesized vinyl-based and native oligocelluloses catalyzed by CtCdP and (b) the synthesized vinyl glucosides catalyzed by β-glucosidase and cellobiose in 4 wt% NaOD/D_2O.

The average degree of polymerization (DP_n) of the vinyl-based oligocelluloses that equals to the average number of repeating glucosyl units, was obtained from the ^{1}H NMR spectra by comparing the peak integration of both anomeric protons with one of the vinyl protons (see equation 3.1) and the obtained DP_n was in the range of 7.3–8.3, except for OC-EA (see below). The number–average molecular weight (M_n) of the prepared vinyl-based oligocelluloses was determined *via* equation 3.3 and the M_n's are calculated to be between 1300 and 1500 g mol^{-1}, except for OC-EA (see Table 3.1). In addition, the DP_n of native oligocellulose was 6.9, slightly lower than the vinyl-based oligocellulose based on the calculation using equation 3.2. As a result, the M_n of native oligocellulose was also lower than the vinyl-based oligocelluloses.

In the case of OC-EA, the calculated M_n was about 3500 g mol^{-1}, 2.7 times higher than the other vinyl-based oligocelluloses. In our previous report,[33] higher M_n of oligocellulose may be achieved during the enzymatic reaction by lowering the concentration of glucosyl acceptor which leads to lower concentration of the synthesized oligocellulose. Under this condition, the intermolecular hydrogen bond between oligocellulose can be reduced causing less precipitation and partially soluble oligocellulose can have further polymerization. Since this is not the case in this study, an error in peak integration of ^{1}H NMR spectra used in equation 3.1 is the most possible reason for this anomalous result.

The intensity of vinyl proton peaks of OC-EA in Figure 3.3a was much smaller than the intensity of vinyl proton peaks of other vinyl-based oligocelluloses, however, the intensity of internal anomeric proton peaks (H2) of those vinyl-based oligocelluloses was similar. Consequently, the amount of vinyl group of OC-EA is also lower than the other vinyl-based

oligocelluloses but they have a comparable number of glucosyl repeating units. According to equation 3.1, if the amount of anomeric protons is constant but the amount of vinyl protons is decreasing, then the calculated DP_n will increase and the calculated M_n will increase as well. The low amount of vinyl proton of OC-EA is possibly due to fragmentation of the acrylate unit that occurred during the enzymatic reaction.

In order to investigate whether the fragmentation of acrylate units of OC-EA is due to hydrolysis by NaOD during the preparation of ^{1}H NMR samples, ^{1}H NMR experiments of vinyl glucosides in the same conditions as vinyl-based oligocelluloses were performed and the results are shown in Figure 3.3b. Each vinyl glucosides still consisted of one (meth) acrylate/(meth)acrylamide groups after treating the samples in slightly basic condition according to the comparison of peak integration of the anomeric proton (H1) with the vinyl protons (H10, H11). The existing vinyl protons of acrylate units of G-EA indicated that no hydrolysis reaction occurred in the acrylate groups of G-EA as well as OC-EA during ^{1}H NMR experiments.

The MALDI-ToF MS spectra of vinyl-based and native oligocelluloses are depicted in Figure 3.4. The most dominant peaks of MALDI-ToF spectra of vinyl-based and native oligocelluloses were derived from the oligocellulose sequences with a number of repeating glucosyl units from 6 to 10. However, the most dominant peaks of MALDI-ToF spectrum of OC-EA (Figure 3.4b) belong to the oligocellulose sequence with fragmentation on the alpha position of the acrylate unit, supporting the low intensity of the vinyl proton of OC-EA as witnessed from the ^{1}H NMR experiment.

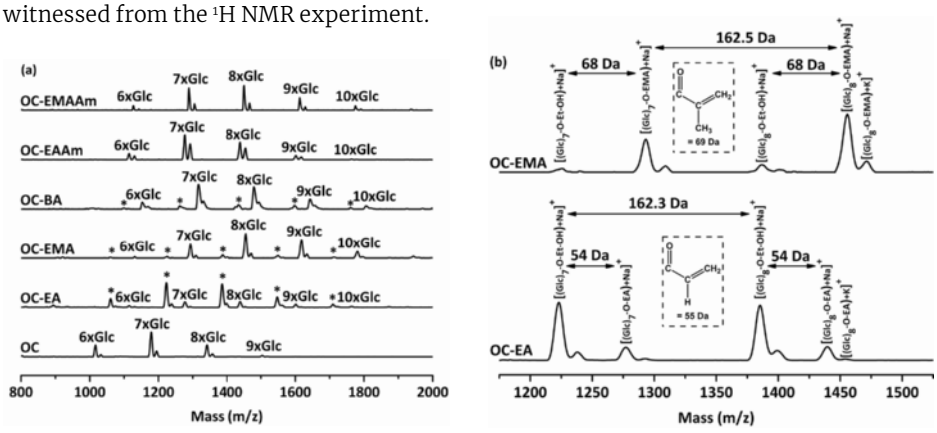

Figure 3.4 (a) MALDI-ToF MS spectra of the synthesized vinyl-based and native oligocelluloses catalyzed by CtCdP. Asterisk symbols in OC-EA, OC-EMA, and OC-BA show the signals that relate to the fragmented oligocelluloses. (b) Magnification of OC-EA and OC-EMA peaks of the MALDI-TOF MS spectra.

Even though the major fragmentation of OC-EA may also be due to the high energy laser irradiation during the MALDI-ToF MS experiments, we should see the same observation in the case of OC-BA since both of them have exactly the same acrylate group. In contrast, only a small amount of fragmented sequences were identified in the spectrum of OC-BA. Additionally, minor fragmentation was also observed in OC-EMA and no fragmentation in OC-EAAm, OC-EMAAm, and native oligocellulose. Therefore, the laser energy might only cause less/no fragmentations. We suggest that this fragmentation phenomena in (meth)acrylate-based oligocelluloses happened due to a nucleophilic substitution of the phosphate ion to the (meth)acrylate groups during the enzymatic synthesis since CtCdP is capable to catalyze the phosphorolysis reaction as well. The proposed mechanism for this phosphorolysis reaction is shown in Scheme 3.2.

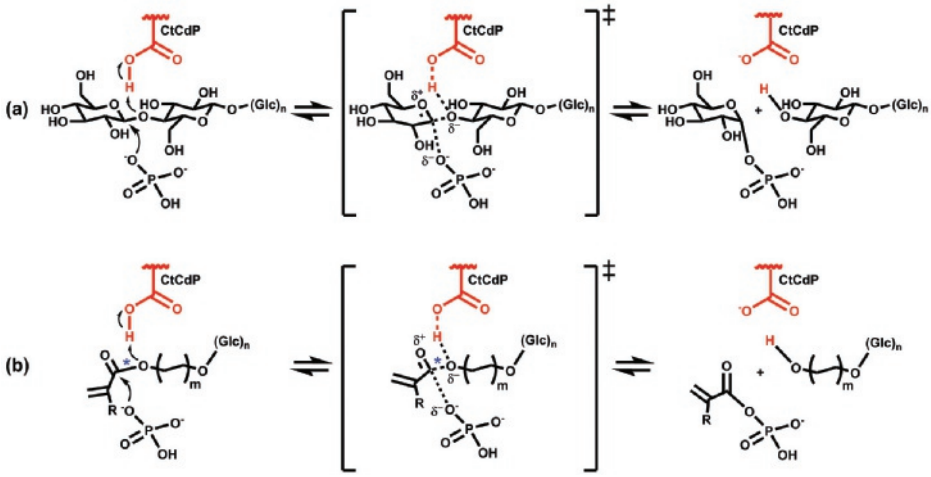

Scheme 3.2 Proposed mechanism of the phosphorolysis reaction of (a) native oligocellulose and (b) (meth)acrylate-based oligocelluloses (R = H, CH_3; m = 1, 2) catalyzed by CtCdP. Asterisk symbols indicate the fragmented bond at the alpha position of the (meth)acrylate groups.

The contrary observation was reported by Freidig *et al.*[55] where methacrylates generally have a higher hydrolysis rate than acrylates at pH 7 in a conventional reaction. Considering the reaction center for hydrolysis and phosphorolysis of (meth)acrylate is exactly the same, it seems that the phosphorolysis in the enzymatic reaction also depends on the structures of the substrates that lead to different outcomes in comparison with the chemical reaction. The difference between the alkyl groups in the substrates (hydrogen *vs* methyl for G-EA and G-EMA; ethyl *vs* butyl for G-EA and G-BA) results in a different reactivity in the enzyme catalyzed phosphorolysis reaction. Furthermore, no fragmentation was discovered in the spectra of OC-EAAm and OC-EMAAm because of the (meth)acrylamide groups are well-known to be more stable towards nucleophilic substitution than (meth)acrylate groups.

Indeed, the study on the selectivity of this enzyme with different substrate structures would be more comprehensive using a structural approach. The x-ray crystal structure of CtCdP was published recently[56] and we will use them to analyze the enzyme selectivity with our substrates in the future.

M_n, M_w, and $Đ$ of the synthesized vinyl-based and native oligocelluloses can be obtained from the MALDI-ToF spectra by equation 3.4–3.6, respectively. The resulted M_n, M_w, and $Đ$ are shown in Table 3.1. The M_n was used to calculate the DP_n *via* equation 3.3 and the numbers were in the range of 7.1–8.9, similar with the DP_n gained from ^{1}H NMR experiments.

SEC was also employed to determine M_n, M_w, and $Đ$ of the vinyl-based and native oligocelluloses and the chromatograms are shown in Figure 3.5. Refractive index signals with a relatively narrow peak and unimodal distribution were observed for all vinyl-based and native oligocelluloses implying that the samples have a low dispersity (Table 3.1), resembling the results from MALDI-ToF experiments very well. The low dispersity of the vinyl-based and native oligocelluloses suggest that a controlled polymerization of the glucosyl units was accomplished in a chain-growth manner – whereby the reaction was initiated at the non-reducing end of the glucosyl acceptor.

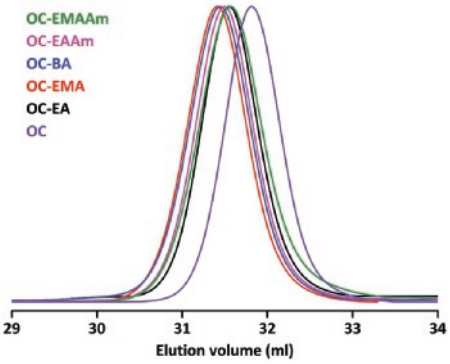

Figure 3.5 SEC measurements (RI signals) of the synthesized vinyl-based and native oligocelluloses catalyzed by CtCdP.

The M_n and M_w were calculated using conventional calibration with pullulan was used as the standard. Both samples and standard have similarity in term of their linear structure that consists of glucosyl unit. The acquired M_n's of the vinyl-based oligocelluloses were in the range of 1385–1512 g mol^{-1} and the numbers were comparable with the previous characterizations. In addition, the elugram of OC-EA was on the same elution volume range with the other oligocelluloses indicating its M_n that was also close to the rest of the products, verifying inaccuracy of the calculated M_n of OC-EA from ^{1}H NMR measurement.

SEC determines the molecular weight of polymers based on the hydrodynamic volume of the polymers in solution. Different polymers with similar hydrodynamic volume will produce similar elution volume. According to our result, it is obvious that different types of vinyl functionalities available as the end group do not result in a significant influence on the differences of the hydrodynamic volume of the synthesized vinyl-based oligocelluloses. Furthermore, the elugram of the native oligocellulose has a slightly higher elution volume than the vinyl-based oligocelluloses meaning that the M_n of the native oligocellulose determined by SEC is lower than the vinyl-based ones, in agreement with the result obtained from ^{1}H NMR and MALDI-ToF experiments (see Table 3.1).

WAXD experiments were performed to determine the crystal type of the synthetic vinyl-based and native oligocelluloses. Cellulose exists in several crystal lattices namely cellulose I, II, III, and IV where each polymorph has different unit cell parameters.[57] WAXD profile of both vinyl-based and native oligocelluloses (Figure 3.6) exhibits exactly the same pattern with three reflection peaks at 2θ of around 12.2° (d = 7.26 Å), 19.8° (d = 4.48 Å), and 22.0° (d = 4.04 Å). A similar observation was also reported in the literature.[31,35] This result concludes that our vinyl-based and native oligocelluloses follow the cellulose II polymorph, the most thermodynamically stable form of crystalline cellulose. The ordered structure of the synthesized oligocelluloses is a result of the strong intermolecular hydrogen bond during enzymatic synthesis. Furthermore, it is shown that different types of end group functionalities do not affect the crystal lattice of the oligocelluloses.

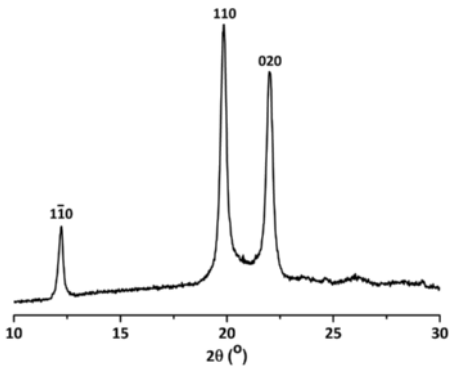

Figure 3.6 WAXD profile of the synthesized vinyl-based and native oligocelluloses catalyzed by CtCdP.

3.4 Conclusions

We have successfully synthesized five types of well-defined vinyl-based oligocelluloses catalyzed by CtCdP in buffer solution. The enzymatic synthesis was followed by TLC and the products were identified at a retardation factor of 0.63. The optimum product formation was reached when the concentration of glucosyl donor is twenty-fold of the glucosyl acceptors. The prepared vinyl-based oligocelluloses possess DP_n and M_n of 7.3–8.9 and 1310–1553 g mol^{-1}, respectively, according to ^{1}H NMR, MALDI-ToF MS, and SEC measurements. Fragmentation phenomena at the alpha position of (meth)acrylate units was observed in OC-EA, OC-EMA, and OC-BA but this observation was absent in OC-EAAm, OC-EMAAm, and native OC. Furthermore, based on the WAXD experiments the synthesized vinyl-based and native oligocelluloses belong to the cellulose II polymorph.

The synthesis of vinyl-based oligocelluloses and the precursors were successfully conducted through eco-friendly pathways. In addition, the CtCdP was presented to have substrate promiscuity with different vinyl glucosides other than its natural substrate. Unfortunately, the commercial availability of CtCdP, the loss of CtCdP during purification, and the cost of the glucosyl donor, α-Glc1*P*, are still challenges for future commercialization. Moreover, further experiments will be directed to prepare the (co)polymers of these vinyl-based oligocelluloses and to study their application for thermoresponsive materials, novel biobased surfactants, and so forth. In order to improve the solubility of oligocelluloses in solution, ionic liquids may be used as suitable green solvents.[58]

3.5 References

1 D. Klemm, H.-P. Schmauder and T. Heinze, in *Biopolymers, Vol. 6 Polysaccharides II: Polysaccharides from Eukaryotes*, eds. S. De Baets, E. Vandamme and A. Steinbüchel, Wiley-VCH Verlag GmbH & Co. KGaA, Weinheim, 1st edn., **2002**, pp. 275–319.

2 H. Nakajima, P. Dijkstra and K. Loos, *Polymers (Basel).*, **2017**, *9*, 1–26.

3 R. J. Moon, A. Martini, J. Nairn, J. Simonsen and J. Youngblood, *Chem. Soc. Rev.*, **2011**, *40*, 3941–3994.

4 T. Huber, J. Müssig, O. Curnow, S. Pang, S. Bickerton and M. P. Staiger, *J. Mater. Sci.*, **2012**, *47*, 1171–1186.

5 T. Yates, A. Ferguson, B. Binns and R. Hartless, *Cellulose-based building materials : Use, performance and risk*, Buckinghamshire, **2013**.

6 T. Watanabe, *Cellul. Commun.*, **1998**, *5*, 91–97.

7 M. Satouchi, T. Watanabe, S. Wakabayashi, K. Ohokuma, T. Koshijima and M. Kuwahara, *J. Japan Soc. Nutr. Food Sci.*, **1996**, *49*, 143–148.

8 European Patent, EP1930012 A1, **2008**.

9 S. I. Mussatto and I. M. Mancilha, *Carbohydr. Polym.*, **2007**, *68*, 587–597.

10 H. Kamitakahara, F. Nakatsubo and D. Klemm, *Cellulose*, **2007**, *14*, 513–528.

11 M. Hato, H. Minamikawa, K. Tamada, T. Baba and Y. Tanabe, *Adv. Colloid Interface Sci.*, **1999**, *80*, 233–270.

12 E. Billès, K. N. Onwukamike, V. Coma, S. Grelier and F. Peruch, *Carbohydr. Polym.*, **2016**, *154*, 121–128.

13 Y. Enomoto-Rogers, H. Kamitakahara, A. Yoshinaga and T. Takano, *Cellulose*, **2010**, *17*, 923–936.

14 Y. Enomoto-Rogers, H. Kamitakahara, A. Yoshinaga and T. Takano, *Cellulose*, **2011**, *18*, 929–936.

15 J. Wang, J. Niu, T. Sawada, Z. Shao and T. Serizawa, *Biomacromolecules*, **2017**, *18*, 4196–4205.

16 E. Billès, V. Coma, F. Peruch and S. Grelier, *Polym. Int.*, **2017**, *66*, 1227–1236.

17 R. Xiao and M. W. Grinstaff, *Prog. Polym. Sci.*, **2017**, *74*, 78–116.

18 F. Nakatsubo, H. Kamitakahara and M. Hori, *J. Am. Chem. Soc.*, **1996**, *118*, 1677–1681.

19 H. Kamitakahara, F. Nakatsubo and D. Klemm, *Cellulose*, **2006**, *13*, 375–392.

20 K. Loos, Ed., *Biocatalysis in Polymer Chemistry*, Wiley-VCH Verlag GmbH & Co. KGaA, Weinheim, 1st edn., **2010**.

21 A. R. A. Palmans and A. Heise, Eds., *Enzymatic Polymerisation*, Springer-Verlag Berlin Heidelberg, Heidelberg, 1st edn., **2011**.

22 S. Shoda, H. Uyama, J. Kadokawa, S. Kimura and S. Kobayashi, *Chem. Rev.*, **2016**, *116*, 2307–2413.

23 C. Fodor, M. Golkaram, J. van Dijken, A. Woortman and K. Loos, *Polym. Chem.*, **2017**, *8*, 6795–6805.

24 S. Egusa, T. Kitaoka, M. Goto and H. Wariishi, *Angew. Chemie - Int. Ed.*, **2007**, *46*, 2063–2065.

25 S. Kobayashi, K. Kashiwa, T. Kawasaki and S. I. Shoda, *J. Am. Chem. Soc.*, **1991**, *113*, 3079–3084.

26 S. Fort, V. Boyer, L. Greffe, G. J. Davies, O. Moroz, L. Christiansen, M. Schülein, S. Cottaz and H. Driguez, *J. Am. Chem. Soc.*, **2000**, *122*, 5429–5437.

27 V. Puchart, *Biotechnol. Adv.*, **2015**, *33*, 261–276.

28 E. C. O'Neill and R. A. Field, *Carbohydr. Res.*, **2015**, *403*, 23–37.

29 H. Nakai, M. Kitaoka, B. Svensson and K. Ohtsubo, *Curr. Opin. Chem. Biol.*, **2013**, *17*, 301–309.

30 T. Serizawa, M. Kato, H. Okura, T. Sawada and M. Wada, *Polym. J.*, **2016**, *48*, 539–544.

31 M. Hiraishi, K. Igarashi, S. Kimura, M. Wada, M. Kitaoka and M. Samejima, *Carbohydr. Res.*, **2009**, *344*, 2468–2473.

32 H. Nakai, M. A. Hachem, B. O. Petersen, Y. Westphal, K. Mannerstedt, M. J. Baumann, A. Dilokpimol, H. A. Schols, J. O. Duus and B. Svensson, *Biochimie*, **2010**, *92*, 1818–1826.

33 D. M. Petrović, I. Kok, A. J. J. Woortman, J. Ćirić and K. Loos, *Anal. Chem.*, **2015**, *87*, 9639–9646.

34 T. Sawano, W. Saburi, K. Hamura, H. Matsui and H. Mori, *FEBS J.*, **2013**, *280*, 4463–4473.

35 Y. Yataka, T. Sawada and T. Serizawa, *Chem. Commun.*, **2015**, *51*, 12525–12528.

36 T. Nohara, T. Sawada, H. Tanaka and T. Serizawa, *Langmuir*, **2016**, *32*, 12520–12526.

37 T. Nohara, T. Sawada, H. Tanaka and T. Serizawa, *J. Biomater. Sci. Polym. Ed.*, **2017**, *28*, 925–938.

38 Y. Yataka, T. Sawada and T. Serizawa, *Langmuir*, **2016**, *32*, 10120–10125.

39 W. M. J. Kloosterman, S. Roest, S. R. Priatna, E. Stavila and K. Loos, *Green Chem.*, **2014**, *16*, 1837–1846.

40 A. Adharis, D. Vesper, N. Koning and K. Loos, *Green Chem.*, **2018**, *20*, 476–484.

41 R. Beerthuis, G. Rothenberg and N. R. Shiju, *Green Chem.*, **2015**, *17*, 1341–1361.

42 J. C. Lansing, R. E. Murray and B. R. Moser, *ACS Sustain. Chem. Eng.*, **2017**, *5*, 3132–3140.

43 A. K. Beine, P. J. C. Hausoul and R. Palkovits, in *Chemicals and Fuels from Bio-Based Building Blocks*, eds. F. Cavani, S. Albonetti, F. Basile and A. Gandini, Wiley-VCH Verlag GmbH & Co. KGaA, Weinheim, 1st edn., **2016**, pp. 245–270.

44 K. J. De France, T. Hoare and E. D. Cranston, *Chem. Mater.*, **2017**, *29*, 4609–4631.

45 Y. Hata, T. Kojima, T. Koizumi, H. Okura, T. Sakai, T. Sawada and T. Serizawa, *ACS Macro Lett.*, **2017**, *6*, 165–170.

46 Y. Cao and H. Li, *Eur. Polym. J.*, **2002**, *38*, 1457–1463.

47 Y. Enomoto-Rogers, H. Kamitakahara, A. Yoshinaga and T. Takano, *Cellulose*, **2011**, *18*, 1005–1014.

48 S. Yagi, N. Kasuya and K. Fukuda, *Polym. J.*, **2010**, *42*, 342–348.

49 I. Otsuka, C. Travelet, S. Halila, S. Fort, I. Pignot-Paintrand, A. Narumi and R. Borsali, *Biomacromolecules*, **2012**, *13*, 1458–1465.

50 M. Sakaguchi, T. Ohura and T. Iwata, in *Functional Materials from Renewable Sources*, eds. F. Liebner and T. Rosenau, American Chemical Society, **2012**, vol. 1107, pp. 133–147.

51 H. Kamitakahara, A. Baba, A. Yoshinaga, R. Suhara and T. Takano, *Cellulose*, **2014**, *21*, 3323–3338.

52 M. Kitaoka and K. Hayashi, *Trends Glycosci. Glycotechnol.*, **2002**, *14*, 35–50.

53 G. Hai Tran, T. Desmet, M. R. M. De Groeve and W. Soetaert, *Biotechnol. Prog.*, **2011**, *27*, 326–332.

54 H. G. Tran, T. Desmet, K. Saerens, H. Waegeman, S. Vandekerckhove, M. D'hooghe, I. Van Bogaert and W. Soetaert, *Bioresour. Technol.*, **2012**, *115*, 84–87.

55 A. P. Freidig, H. J. M. Verhaar and J. L. M. Hermens, *Environ. Toxicol. Chem.*, **1999**, *18*, 1133–1139.

56 E. C. O'Neill, G. Pergolizzi, C. E. M. Stevenson, D. M. Lawson, S. A. Nepogodiev and R. A. Field, *Carbohydr. Res.*, **2017**, *451*, 118–132.

57 J.-L. Wertz, O. Bédué and J. P. Mercier, *Cellulose Science and Technology*, EPFL Press, Laussane, 1st edn., **2010**.

58 H. Wang, G. Gurau and R. D. Rogers, *Chem. Soc. Rev.*, **2012**, *41*, 1519–1537.